Int J Clin Exp Med 2019;12(7):8579-8585
www.ijcem.com /ISSN:1940-5901/IJCEM0093757

Original Article

The protective effect of catalpol on respiratory syncytial virus infection

Pengwei Wang[1], Jiahai Yu[1], Li Zhou[2], Baozhu Yue[1], Meijuan Liu[3]

[1]Department of Pediatrics, Weifang Maternal and Child Health Hospital, Weifang, Shandong, China; [2]Department of Pathology, Weifang Maternal and Child Health Hospital, Weifang, Shandong, China; [3]Department of Respiratory, Affiliated Hospital of Weifang Medical University, Weifang, Shandong, China

Received March 13, 2019; Accepted May 13, 2019; Epub July 15, 2019; Published July 30, 2019

Abstract: Respiratory syncytial virus (RSV) infection can cause severe bronchiolitis, pneumonia or even death in infants, or induce childhood asthma. Currently no specific drug is available for RSV infection. With multiple pathology roles, catalpol has significant roles in anti-oxidation and anti-infection, but has not been studied in RSV infection. This study aimed to investigate the effects and mechanism of catalpol on RSV infection via establishing a mouse RSV infection model, further illustrating the effect of catalpol on RSV infection and providing evidences for clinical treatment. BALB/c mice were used to generate a RSV infection model using intranasal drops of viral solutions, and mice were then treated with 5 mM or 10 mM catalpol. Real-time fluorescent quantitative PCR was used to measure RSV load in mouse pulmonary tissues, while ELISA was used to quantify expression of inflammatory factors including TNF-α and IL-1β. Real-time PCR and Western blot were used to test cellular expression of NF-κB (p65) mRNA and protein expression. ROS and SOD activity in all cells were analyzed. Compared to the control group, RSV infected mice had higher RSV load in pulmonary tissues, elevated serum TNF-α and IL-1β levels, expression of NF-κB mRNA and protein, higher ROS contents and lower SOD activity ($p < 0.05$). Catalpol can decrease RSV load and ROS contents, elevate SOD activity, decrease NF-κB mRNA and protein expressions, and suppress TNF-α and IL-1β levels ($p < 0.05$ compared to model group) in a dose-dependent manner. Catalpol can exert anti-RSV infection roles via modulating oxidation/anti-oxidation balance and inhibiting inflammation progression.

Keywords: Catalpol, respiratory syncytial virus, anti-oxidation, NF-κB, inflammatory factor

Introduction

Respiratory syncytial virus (RSV) was firstly identified in nasopharyngeal secretion of a chimpanzee having a respiratory infection, and was classified into Pneumovirus genus of Paramyxivirinae family, including both RSV type A and type B [1, 2] RSV is one single stranded negative RNA virus without segmentation and capsules, with virus-coding transmembrane protein on the membrane [3]. RSV infection can cause various respiratory diseases including bronchiolitis, laryngitis, pneumonia and bronchiolitis [4, 5]. RSV infection can cause severe bronchiolitis in infants, or induce childhood refractory asthma, or even cause pneumonia and death, thus becoming a common pediatric disease [6]. Catalpol has multiple pathological roles including significant anti-oxidation and anti-inflammation [7, 8]. However, its effect on RSV infection has not been studied. This study aimed to investigate the function and mechanism of catalpol on RSV infection via establishing a mouse RSV infection model, further illustrating the effect of catalpol on RSV infection, and providing evidence for clinical treatment of RSV infection.

Materials and methods

Experimental animals

Healthy male BALB/c mice (4 weeks old, SPF grade, body weight 20 ± 2 g) were purchased from laboratory animal center of Shandong University and were kept in an SPF grade animal facility with fixed temperature (21 ± 1°C) and relative humidity (50-70%) under a 12 h light-dark cycle.

Mice were used for all experiments and all procedures were approved by the Animal Ethics

Committee of Weifang Maternal and Child Health Hospital.

Major equipment and reagents

Catalpol was purchased from Biological Product Institute of China. RSV nucleic acid test kit was purchased from Zhijiang Biotech (China). RSV stock was kept in-house. Hep-2 cell line was obtained from ATCC cell bank (US). DMEM culture medium, fetal bovine serum (FBS) and streptomycin-penicillin were purchased from Hyclone (US). Enzyme linked immunosorbent assay (ELISA) kit for tumor necrosis factor (TNF)-α and interleukin (IL)-1β were obtained from R&D (US). SOD activity kit was purchased from Cell Signaling (US). PVDF membrane was purchased from Pall Life Sciences (US). Chemical reagents for Western blotting were purchased from Beyotime (China). ECL kit was purchased from Amersham Biosciences (US). Rabbit anti-mouse NF-κB monoclonal antibody, and goat anti-rabbit horseradish peroxidase (HRP) conjugated IgG antibody were obtained from Cell Signaling (US). RNA extraction kit and reverse transcription kit were purchased from Axygen (US). Other common reagents were purchased from Sangon (China). Labsystem Version 1.3.1 microplate reader was purchased from Bio-rad (US). Ultrapure workstation was purchased from Sutai (China). DNA amplification cycler (Gene Amp PCR System 2400) was purchased from PE (US).

Animal grouping and treatment

BALB/c mice were randomly assigned into four groups: control group, model group, which received intranasal drops of RSV solution to generate a mouse RSV infection model, and 5 mM or 10 mM catalpol groups, which received intraperitoneal injection of 5 mM or 10 mM catalpol 30 min after model generation.

Mouse RSV infection model preparation

Mouse RSV infection model was generated by intranasal drops of RSV solutions according to previous literature [9]. RSV solution was first prepared. In brief, Hep-2 cells were resuscitated in 37°C water bath until complete thawing. Cells were then centrifuged at 1000 rpm for 3 min, and were added into 0.9 ml fresh medium containing 2% FBS. 0.1 ml thawed viral solution was then inoculated and mixed to completely cover the cell surface. After absorbance for 90 min, cell maintenance buffer was added for 72 h culture. When 80% of cells had cytotoxic effects, cell suspensions were collected, and repeatedly frozen (-80°C) and thawed (37°C) three times. Cell mixture was then centrifuged at 2500 rpm for 10 min. The precipitation was then discarded to collect the supernatant, which contains RSV particles at 2×10^8 PFU/ml titer. Mice were anesthetized by 3 ml/kg 1% pentobarbital via intraperitoneal injection. 100 μl RSV solutions were then slowly applied bilaterally into the nose during animal inhalation. Mouse body was kept in a vertical position with the head bending backward for 1 min to ensure the entry of RSV into trachea and bronchi. Nose dropping was performed daily for two consecutive days.

Sample collection

24 h after processing, a 1 ml venous blood sample was collected from the tail vein of all mice. The control group was also collected for blood samples. Blood was centrifuged at 3000 rpm for 15 min to collect serum, which was stored in a -80°C fridge for further use. Mice were then sacrificed to collect the left pulmonary tissues, which were kept in a -80°C fridge for further use.

Real-time PCR for RSV load in mouse pulmonary tissues

Under sterile condition, pulmonary tissues were rinsed in PBS and were homogenized by liquid nitrogen. RZ lysis buffer was added for preparing the homogenate. Nucleic acid was extracted by 12,000 rpm centrifugation for 5 min at 4°C, and the addition of chloroform and ethanol, followed by 12,000 rpm centrifugation at 4°C for 30 s. Viral extraction kit was used to extract RNA. RSC nucleic acid test kit was used to quantify viral load in all groups.

ELISA for TNF-α and IL-1β expression level

All samples were tested for TNF-α and IL-1β levels in mouse serum using ELISA kit following the instruction of test kits. In brief, a 96-well plate was loaded with 50 μl serially diluted samples, which were used to plot standard curves. 50 μl test samples were then added into test wells in triplicates. After washing 5 times, liquids were discarded, and filled with

Table 1. Primer synthesis sequence

Target gene	Forward primer 5'-3'	Reverse primer 5'-3'
GAPDH	AGTGCCAGCCTCGTCTCATAG	ACTTGCAACTTGCCGTGGGTAG
NF-κB	CTCATCGAATAAGCGCAATGG	GCACTCTTAGCGCGTAGC

washing buffer for 30 sec of vortex. The rinsing procedure was repeated 5 times. 50 μl enzyme labelling reagent was then added into each well except the blank control. After gentle mixture, the wells were incubated for 30 min at 37°C. Chromogenic substrates A and B were sequentially added (50 μl each), followed by 37°C dark incubation for 10 min. The test plate was then mixed with 50 μl quenching buffer as the blue color turned into yellow. Using the blank control well as the reference, OD values at 450 nm wavelength were measured by a microplate reader within 15 min after adding quenching buffer. Linear regression model was then plotted based on the concentration of standard samples and respective OD values. Sample concentration was further deduced based on OD values and regression function.

Real-time PCR for NF-κB mRNA expression in pulmonary tissues

Under sterile condition, pulmonary tissues were rinsed by PBS and homogenized in liquid nitrogen. Trizol reagent was used to extract mRNA. cDNA was synthesized based on specific PCR primers (**Table 1**). Real-time PCR was then employed to test target gene expression under the following conditions: 52°C 1 min, followed by 35 cycles each containing 90°C 30 s, 58°C 50 s and 72°C 35 s. Fluorescent quantitative PCR cycler software was used to collect relevant data for calculating CT values based on the internal reference GAPDH gene. Standard curve was plotted for semi-quantitative analysis by $2^{-\Delta Ct}$ method.

Western blot for NF-κB protein expression level

Pulmonary tissues were mixed with lysis buffer for an iced incubation for 15~30 min. After ultrasound treatment (5 s, 4 times), the mixture was centrifuged at 10,000 g for 15 min. The supernatant was saved, quantified, and stored at -20°C for Western blotting assay. Proteins were separated in 10% SDS-PAGE, and were transferred to PVDF membrane by semi-dry method (160 mA, 1.5 h). Non-specific background was removed by 5% nonfat milk powder for a 2-hour incubation at room temperature. Primary antibody against NF-κB (1:1,000 dilutions) was added for 4°C overnight incubation. After PBST washing, goat anti-rabbit secondary antibody (1:2,000) was then added for dark incubation at room temperature for 30 min. ECL reagent was then used to develop the membrane for 1 min, followed by X-ray exposure and observation. Protein imaging system and Quantity One software was then applied to scan X-ray films and band density. Each experiment was repeated four times (N = 4) for the ease of statistical analysis.

SOD activity and ROS content assay in pulmonary tissues

Using SOD activity assay kit, SOD activity was tested in intestinal tissues following the manual instructions. In brief, tissues were denatured at 95°C for 40 min, and were centrifuged at 4,000 rpm for 10 min after cooling down. Ethanol-chloroform mixture (5:3, v/v) was used to extract the ethanol phase in the homogenate for total SDO activity assay. Cells were denatured at 95°C for 40 min, rinsed in cold water, and were centrifuged at 4,000 rpm for 10 min. At 37°C, homogenates were incubated in 2',7'-dichlorofluorescein diacetate (DCF-DA) for 15 min. After centrifugation at 10,000 rpm for 15 min, the precipitations were re-suspended in sterilized PBS buffer, and were incubated at 37°C for 60 min. Spectrometry was used to detect the ROS levels expressed as ROS production percentage.

Statistical analysis

SPSS 16.0 software was used to analyze all data, of which measurement data were expressed as mean ± standard deviation (SD). Analysis of variance (ANOVA) was used to compare means across groups. A statistical significance was defined when $p < 0.05$.

Results

Effects of catalpol on RSV loading of mouse pulmonary tissues

RSV loading was significantly elevated in the model group ($p < 0.05$ compared to control group). After catalpol treatment, RSV loading

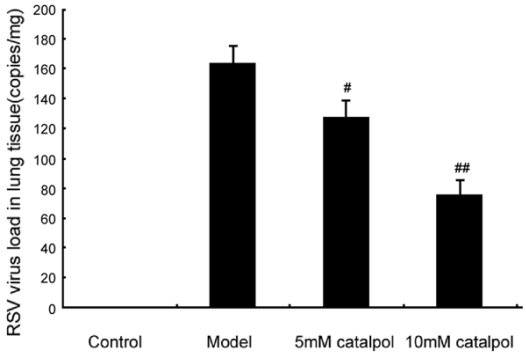

Figure 1. Effects of catalpol on RSV loading in infected mouse pulmonary tissues. #p < 0.05, ##p < 0.01 compared to model group.

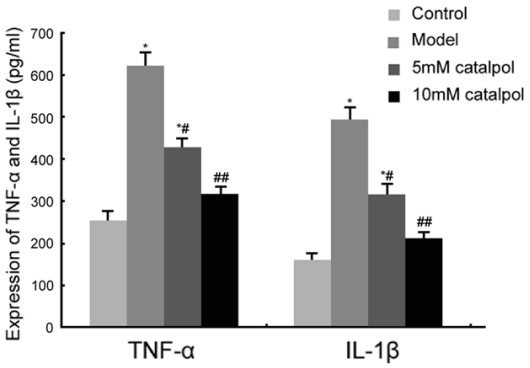

Figure 2. Effects of catalpol on serum expression of inflammatory factor TNF-α and IL-1β. *p < 0.05 compared to control group; #p < 0.05, ##p < 0.01 compared to model group.

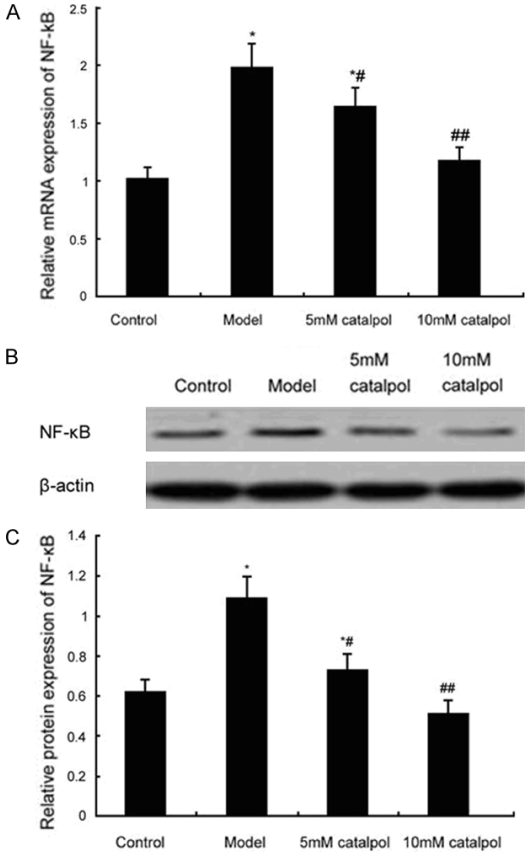

Figure 3. Effects of catalpol on pulmonary expression of NF-κB. Total RNA or protein was isolated followed by measuring NF-κB mRNA expression (A) or protein expression (B and C). *p < 0.05 compared to control group; #p < 0.05, ##p < 0.01 compared to model group.

increase was significantly suppressed in a dose-dependent manner (p < 0.05 compared to the model group, **Figure 1**).

Catalpol effects on serum expression of inflammatory factors TNF-α and IL-1β

ELISA was used to test the expression of serum inflammatory factors TNF-α and IL-1β in all groups. Results showed significantly enhanced serum inflammatory factors TNF-α and IL-1β (p < 0.05 compared to control group). Catalpol treatment significantly suppressed serum inflammatory factors TNF-α and IL-1β in a dose-dependent manner (p < 0.05 compared to model group, **Figure 2**).

Catalpol effects on pulmonary expression of NF-κB mRNA

Real time PCR was used to test the effect of catalpol on NF-κB mRNA expression in mouse pulmonary tissues. Results showed significantly enhanced NF-κB mRNA expression in the RSV infected model mice (p < 0.05 compared to control group). Catalpol treatment significantly suppressed NF-κB mRNA expression in a dose-dependent manner (p < 0.05 compared to the model group, **Figure 3**).

Effects of catalpol on NF-κB protein expression in pulmonary tissues

Western blot was used to test the effect of catalpol on NF-κB protein expression in mouse pulmonary tissues. Results showed significantly enhanced NF-κB protein expression in RSV infected model mice (p < 0.05 compared to control group). Catalpol treatment significantly suppressed NF-κB protein expression in a dose-dependent manner (p < 0.05 compared to model group). 10 mM catalpol had more potent inhibiton effects but without statistically

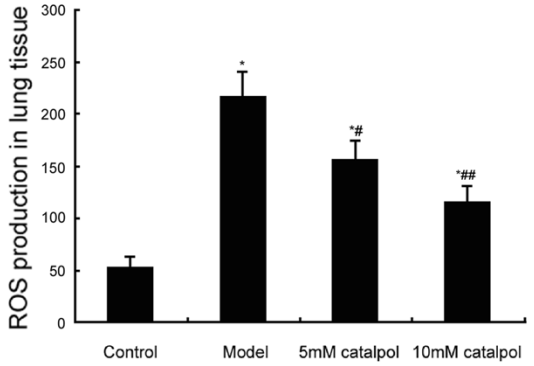

Figure 4. Effects of catalpol on pulmonary ROS production in mouse. *p < 0.05 compared to control group; #p < 0.05, ##p < 0.01 compared to model group.

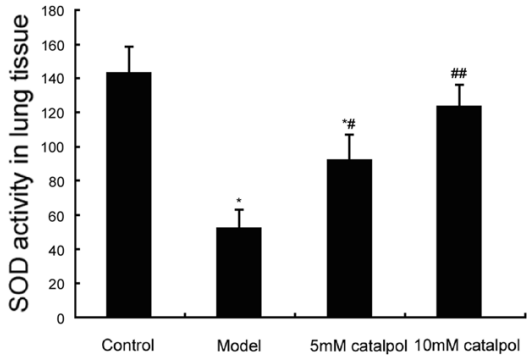

Figure 5. Effects of catalpol on SOD activity in mouse pulmonary tissues. *p < 0.05 compared to control group; #p < 0.05, ##p < 0.01 compared to model group.

significantly difference compared to control group (**Figure 3**).

Effects of catalpol on ROS productivity in mouse pulmonary tissues

We further tested the effect of catalpol on ROS production in mouse pulmonary tissues. Results showed significantly elevated ROS production in RSV infection model mice ($p < 0.05$ compared to control group). Catalpol treatment significantly depressed ROS production in pulmonary tissues ($p < 0.05$ compared to model group, **Figure 4**) in a dose-dependent manner.

Effects of catalpol on mouse pulmonary SOD activity

We further tested the effect of catalpol on SOD activity in mouse pulmonary tissues. Results showed significantly depressed SOD activity in RSV infection model mice ($p < 0.05$ compared to control group). Catalpol treatment significantly recovered SOD activity in pulmonary tissues ($p < 0.05$ compared to model group, **Figure 5**) in a dose-dependent manner.

Discussion

RSV can affect populations at all age groups, especially for those with compromised immune functions. It can cause upper or lower respiratory tract infection, and can lead to recurrent infections in short term [10, 11]. RSV has high incidences, as more than 60% of infants under 1 year old had RSV infection, and more than 80% children under 2 years age had infection. The recurrent rate can be every three years [12]. RSV infection can also cause variable inflammation, and hyperactivity in the airway tract [10]. Various factors including immunity, environment and nutrition status can affect RSV infection pathogenesis, which lacks specific drug treatments [13, 14]. The pathology process of RSV infection includes energy expenditure, free radical production and inflammation [15]. A previous study found that injury of oxidative stress during RSV infection can disrupt the body's oxidation/anti-oxidation balance, thus producing large amounts of ROS) to change the body's immune status [16]. Therefore the identification of effective drugs is critical for treating RSV infection.

Catalpol is one effective compound extracted from tradition Chinese medicine radix rehmanniae, and is one iridoid glucoside compound with small molecular weight [17]. Previous studies showed various biological activities of catalpol including anti-tumor, anti-fungal, anti-viral, anti-Alzheimer's disease, inhibiting the permeability of micro vessels, and anti-inflammation [18, 19]. The function and mechanism of catalpol against RSV infection, however, has not been illustrated. This study thus established a RSV infected mouse model, which received catalpol treatment, in order to analyze the role and mechanism of catalpol on RSV infection. Our results showed elevated RSV loading in infected mouse pulmonary tissues. Catalpol treatment can decrease RSV loading in a dose-dependent manner, suggesting satisfactory treatment effects on RSV infection.

Further analysis of the mechanism for anti-RSV infection by catalpol demonstrated elevated serum expressions of TNF-α and IL-1β, plus

higher ROS contents and lower SOD activity in pulmonary tissues in RSV infection mice. When the body is under oxidative stress condition, over-production of free radicals such as ROS may exceed the clearance potency of the body's anti-oxidation system, leading to dynamic imbalance of the oxidation/anti-oxidation system, further causing tissue inflammation and injury. Therefore, the body's oxidative/reductive status is closely correlated with disease onset [20]. The disruption of the body's oxidation/anti-oxidation system produces large amounts of oxygen free radicals such as ROS, superoxide anion, and hydroxyl free radicals. The decrease of the anti-oxidase system may cause over-oxidation of pulmonary lipids, DNA structural/functional injury and cell apoptosis [21, 22]. Pulmonary tissue injury may release large amounts of inflammatory factors. Nuclear factor kappa B (NF-κB) is mainly involved in the body's defense reaction, tissue injury and stress, cell differentiation, apoptosis and signal transduction during tumor growth inhibition. Under viral infection, it's expression may be significantly elevated, further disrupting the body's pro-inflammatory/anti-inflammatory balance, thus aggravating tissue injury [23]. The application of catalpol at different dosages can decrease ROS contents and increase SOD activity in a dose-dependent manner, further accelerating the recovery of oxidation/antioxidation system, decreasing secretion of inflammatory factors TNF-α and IL-1β, and improving inflammation, eventually exerting anti-RSV infection role.

Conclusion

Catalpol can inhibit inflammation progression and fight against RSV infection via modulating oxidation/anti-oxidation balance. This study provides a novel drug choice and theoretical evidence for clinical treatment of RSV infection.

Disclosure of conflict of interest

None.

Address correspondence to: Dr. Meijuan Liu, Department of Respiratory, Affiliated Hospital of Weifang Medical University, No.2428, Yuhe Road, Kuiwen District, Weifang 261031, Shandong, China. Tel: +86-0536-8068903; Fax: +86-0536-8068903; E-mail: dengbeireng1555@126.com

References

[1] Berry CE, Billheimer D, Jenkins IC, Lu ZJ, Stern DA, Gerald LB, Carr TF, Guerra S, Morgan WJ, Wright AL and Martinez FD. A distinct low lung function trajectory from childhood to the fourth decade of life. Am J Respir Crit Care Med 2016; 194: 607-12.

[2] Torres JP, De la Maza V, Kors L, Villarroel M, Piemonte P, Izquierdo G, Salgado C, Tordecilla J, Contardo V, Farfan MJ, Mejias A, Ramilo O and Santolaya ME. Respiratory viral infections and coinfections in children with cancer, fever and neutropenia: clinical outcome of infections caused by different respiratory viruses. Pediatr Infect Dis J 2016; 35: 949-54.

[3] Caffarelli C, Santamaria F, Di Mauro D, Mastrorilli C, Mirra V and Bernasconi S. Progress in pediatrics in 2015: choices in allergy, endocrinology, gastroenterology, genetics, haematology, infectious diseases, neonatology, nephrology, neurology, nutrition, oncology and pulmonology. Ital J Pediatr 2016; 42: 75.

[4] Napierkowski DB. Diagnosing and treating respiratory syncytial virus bronchiolitis. Nurse Pract 2016; 41: 1-4.

[5] Schuijs MJ, Hartmann S, Selkirk ME, Roberts LB, Openshaw PJ and Schnoeller C. The helminth-derived immunomodulator AvCystatin reduces virus enhanced inflammation by induction of regulatory IL-10+ T Cells. PLoS One 2016; 11: e0161885.

[6] Prill MM, Iwane MK, Little D and Gerber SI. Investigation of respiratory syncytial virus-associated deaths among US children aged < 2 years, 2004-2007. J Pediatric Infect Dis Soc 2016; 5: 333-6.

[7] Xue B, Ma B, Zhang Q, Li X, Zhu J, Liu M, Wu X, Wang C and Wu Z. Pharmacokinetics and tissue distribution of Aucubin, Ajugol and Catalpol in rats using a validated simultaneous LC-ESI-MS/MS assay. J Chromatogr B Analyt Technol Biomed Life Sci 2015; 1002: 245-53.

[8] Wang JM, Yang LH, Zhang YY, Niu CL, Cui Y, Feng WS and Wang GF. BDNF and COX-2 participate in anti-depressive mechanisms of catalpol in rats undergoing chronic unpredictable mild stress. Physiol Behav 2015; 151: 360-8.

[9] Rudd PA, Chen W and Mahalingam S. Mouse and cotton rat models of human respiratory syncytial virus. Methods Mol Biol 2016; 1442: 209-17.

[10] Srinivasa BT, Restori KH, Shan J, Cyr L, Xing L, Lee S, Ward BJ and Fixman ED. STAT6 inhibitory peptide given during RSV infection of neonatal mice reduces exacerbated airway responses upon adult reinfection. J Leukoc Biol 2017; 101: 519-529.

[11] Broadbent L, Villenave R, Guo-Parke H, Douglas I, Shields MD and Power UF. In vitro modeling of RSV infection and cytopathogenesis in well-differentiated human primary airway epithelial cells (WD-PAECs). Methods Mol Biol 2016; 1442: 119-39.

[12] Makris S, Bajorek M, Culley FJ, Goritzka M and Johansson C. Alveolar macrophages can control respiratory syncytial virus infection in the absence of type I interferons. J Innate Immun 2016; 8: 452-63.

[13] Shrivastava P, Sarkar I, Atanley E, Gomis S and van Drunen Littel-van den Hurk S. IL-12p40 gene-deficient BALB/c mice exhibit lower weight loss, reduced lung pathology and decreased sensitization to allergen in response to infection with pneumonia virus of mice. Virology 2016; 497: 1-10.

[14] Mebratu YA, Smith KR, Agga GE and Tesfaigzi Y. Inflammation and emphysema in cigarette smoke-exposed mice when instilled with poly (I:C) or infected with influenza a or respiratory syncytial viruses. Respir Res 2016; 17: 75.

[15] Ren K, Lv Y, Zhuo Y, Chen C, Shi H, Guo L, Yang G, Hou Y, Tan RX and Li E. Suppression of IRG-1 reduces inflammatory cell infiltration and lung injury in respiratory syncytial virus infection by reducing production of reactive oxygen species. J Virol 2016; 90: 7313-7322.

[16] Komaravelli N, Tian B, Ivanciuc T, Mautemps N, Brasier AR, Garofalo RP and Casola A. Respiratory syncytial virus infection down-regulates antioxidant enzyme expression by triggering deacetylation-proteasomal degradation of Nrf2. Free Radic Biol Med 2015; 88: 391-403.

[17] Xu Z, Zhang L, Li X, Jiang Z, Sun L, Zhao G, Zhou G, Zhang H, Shang J and Wang T. Mitochondrial fusion/fission process involved in the improvement of catalpol on high glucose-induced hepatic mitochondrial dysfunction. Acta Biochim Biophys Sin (Shanghai) 2015; 47: 730-40.

[18] Kim DW, Cho JH, Cho GS, Kim IH, Park JH, Ahn JH, Chen BH, Shin BN, Tae HJ, Hong S, Cho JH, Kim YM, Won MH and Lee JC. Hyperthermic preconditioning severely accelerates neuronal damage in the gerbil ischemic hippocampal dentate gyrus via decreasing SODs expressions. J Neurol Sci 2015; 358: 266-75.

[19] Zhu J, Chen X, Wang H and Yan Q. Catalpol protects mice against renal ischemia/reperfusion injury via suppressing PI3K/Akt-eNOS signaling and inflammation. Int J Clin Exp Med 2015; 8: 2038-44.

[20] El-Sahar AE, Safar MM, Zaki HF, Attia AS and Ain-Shoka AA. Neuroprotective effects of pioglitazone against transient cerebral ischemic reperfusion injury in diabetic rats: modulation of antioxidant, anti-inflammatory, and anti-apoptotic biomarkers. Pharmacol Rep 2015; 67: 901-6.

[21] Zhang W, Xing B, Yang L, Shi J and Zhou X. Icaritin attenuates myocardial ischemia and reperfusion injury via anti-inflammatory and anti-oxidative stress effects in rats. Am J Chin Med 2015; 43: 1083-97.

[22] Komaravelli N and Casola A. Respiratory viral infections and subversion of cellular antioxidant defenses. J Pharmacogenomics Pharmacoproteomics 2014; 5.

[23] Harijith A, Ebenezer DL and Natarajan V. Reactive oxygen species at the crossroads of inflammasome and inflammation. Front Physiol 2014; 5: 352.